Available online at www.sciencedirect.com

ScienceDirect

Advances in Space Research 60 (2017) 2452–2463

ADVANCES IN SPACE RESEARCH (a COSPAR publication)

www.elsevier.com/locate/asr

Variation in occurrence of equatorial plasma bubbles (EPBs) using All Sky Imager from low latitude station Kolhapur (16.8 °N, 74.2 °E, 10.6° dip. Lat.)

A.K. Sharma [a], O.B. Gurav [a,*], G.A. Chavan [a], H.P. Gaikwad [a], R.N. Ghodpage [b], P.T. Patil [b]

[a] Space and Earth Science Laboratory, Department of Physics, Shivaji University, Kolhapur, India
[b] Medium Frequency Radar, Indian Institute of Geomagnetism, Shivaji University Campus, Kolhapur, India

Received 30 March 2017; received in revised form 15 August 2017; accepted 10 September 2017
Available online 19 September 2017

Abstract

All Sky Imager (ASI) data of over 351 nights with OI 630.0 nm emission recorded during 2011 to 2015 (increasing phase of 24th solar cycle) are analyzed to study the percentage occurrence of EPBs. The ASI is installed at low latitude station Kolhapur (16.8 °N, 74.2 °E, 10.6° dip. Lat.) which has 140° field of view (FOV). In this paper we have studied hourly, daily, seasonal and yearly percentage of occurrence of EPBs and their variation with solar and magnetic activity. The EPBs onset occurs at around 20:00 IST and extends towards dawn with a peak around midnight. We analyzed all the disturbed nights (Ap > 18) from the period of 2011 to 2015 and observed that the magnetic activity suppresses the occurrence of EPBs. Also the EPBs are fairly correlated with solar activity (10.7 cm solar flux).
© 2017 COSPAR. Published by Elsevier Ltd. All rights reserved.

Keywords: Occurrence of EPBs; All Sky Imager; Solar activity

1. Introduction

The Ionospheric irregularities which cause disturbances in the radio signals have been monitored and studied using different techniques such as ASI (e.g. Sahai et al., 1994; Mukherjee et al., 1998), GPS (L-band scintillation) (e.g. Rama Rao et al., 2006, Haase et al., 2011), VHF scintillation technique (e.g. Chakraborty et al., 1999; Iyer et al., 2006; Chavan et al., 2016) in the past. This Ionospheric irregularity is generated at or near the magnetic equator in the post sunset period and they move upward with respect to ambient plasma in the equatorial ionosphere due to Rayleigh Taylor instability (Sinha et al., 1996). As they grow in altitude, the irregularities expand towards the poles aligning the magnetic field lines and appears as depletions in optical intensity (OI 630.0 nm) as seen in airglow images which are commonly referred to as equatorial plasma bubbles (EPBs) (Makela and Miller, 2008). The OI 630.0 nm emission is produced in the bottom side of the F-region (250–300 km) by the dissociative recombination of O_2^+ with electrons. The reaction mechanism is as given below,

$$O_2^+ + e \rightarrow O + O^* \quad (1)$$

$$O^* \rightarrow O + h\upsilon_{(630.0\ \mathrm{nm})} \quad (2)$$

where * indicates an excited state which is responsible for the ionospheric OI 630.0 nm emission (Pimenta et al., 2001).

* Corresponding author.
E-mail addresses: aks_phy@unishivaji.ac.in (A.K. Sharma), omgurav91@gmail.com (O.B. Gurav), gangadharchavan2@gmail.com (G.A. Chavan), herambgaikwad01@gmail.com (H.P. Gaikwad), rupeshghodpage@gmail.com (R.N. Ghodpage), ptpiigkop@yahoo.com (P.T. Patil).

https://doi.org/10.1016/j.asr.2017.09.014
0273-1177/© 2017 COSPAR. Published by Elsevier Ltd. All rights reserved.

Understanding the daily and seasonal variations in the occurrence of EPBs at a particular location is very important as it causes severe interference and abrupt disruption in trans-ionospheric radio propagation and thus affects the navigation and communication systems (Ghodpage et al., 2014). Recent studies indicate that a suitable condition for EPB growth is bottom side spread F (BSSF) which is a function of the F region dynamo electric field and this field is dependent on magnetic activity and on season (Whalen, 2002). The requirements for R-T instability growth are post sunset rise of the F region, the availability of a seed perturbation to trigger the R-T mechanism and the absence of a strong transequatorial thermospheric wind (Mendillo et al., 1992). Several investigators studied the day to day variability of the occurrence of EPBs during geomagnetically quite and disturbed conditions in the Brazilian sector (e.g. Fagundes et al., 1999; Abalde et al., 2009). Sahai et al. (1994) presented the seasonal variation of occurrence of EPBs recorded by OI 630.0 nm airglow emission at Cachoeira Paulista, Brazil during March 1987–July 1989 (the ascending phase of 22nd solar cycle). Patra et al. (2005), studied the simultaneous observations of ESF irregularities made using 18 MHz radar operated at the equatorial station Trivandrum (77 °E, 8.5 °N, 0.5 °N dip. Lat.) and 53 MHz radar at Gadanki (79.2 °E, 13.5 °N, 12.5 °N dip. Lat.). They found that the spread F irregularities at both the locations are found to occur nearly at the same time but are observed for longer duration at Gadanki that at Trivandrum. Also, Patra et al., (2012) reported first observations of field aligned irregularities (FAIs) made with E-W scanning capability of Gadanki Ionospheric Radar Interferometer (GIRI) and studied its origin, evolution and drift velocity. Taori et al. (2013), reported first measurement of mesospheric waves (using OI 557.7 nm airglow emission) and thermospheric measurements (using OI 630.0 nm airglow emission) recorded using All Sky Imager (ASI) with 150° FOV from Gadanki (13.51 °N, 79.21 °E) and studied the possible linkage of mesospheric waves to F-region plasma depletions. Further, Taori et al. (2015), analyzed an EPB event using multi-station optical data from Kolhapur (16.8 °N, 74.2 °E, 10.6° dip. Lat.), Gadanki (79.2 °E, 13.5 °N, 12.5 °N dip. Lat.) and Ranchi (23.3 °N, 85.3 °E) and observed the tilted E-W wave structures propagating towards the equator and this could be the possible cause behind the observed EPB events over low latitudes of Indian region. Recently, Narayanans et al., (2017) studied the airglow observations carried out from Panhala (16.8 °N, 74.1 °E, 11.1 °N dip. Lat.) station which is very near to Kolhapur. They examined different aspects of EPBs such as drift, Inter depletion distance (IDD), tilt angles etc, to study the evolution of EPBs. These observations were made in low solar activity conditions in year 2008 where they observed the lack of significant PRE determined by Ionosonde Tirunelveli (1.1 °N dip. Lat.). In spite of this the EPBs are observed in All Sky Imager operated at Panhala station. Xiong et al. (2010), studied the EPBs occurrence rate using Challenging Mini-satellite Payload (CHAMP) and Gravity Recovery and Climate Experiment (GRACE) satellites during the years 2001–2009 which lies in 23rd solar cycle and they found that the occurrence rate increases linearly with solar flux at the same rate for both the satellites. Also Kumar (2017) recently studied EPB occurrence rate during the years 2007–2009 using slant TEC data over Indian region and reveals that solar activity influence of EPB occurrence is seasonal dependent with a maximum influence during equinox (0.88) and minimum during winter (0.73).

However, in the past, long time variation in occurrences of EPBs of about five years studied using optical data (ASI 630.0 nm emission) has not been addressed over Indian region. In the present study we have used ASI data recorded from a low latitude station Kolhapur (16.8 °N, 74.2 °E, 10.6° dip. Lat.) with nightglow OI 630.0 nm emission for the period of 2011 to 2015 (the ascending phase of 24th solar cycle). Kolhapur is located in between the dip equator and the northern crest of the equatorial ionization anomaly (EIA) thus it is a unique place to study the electro-dynamical coupling in E and F region using nightglow OI 630.0 nm emission data (Nade et al., 2013). Earlier Sharma et al. (2014) from the same location reported the occurrence of EPBs for the period of October 2010 to May 2012 and observed that the occurrence in equinox season is possibly associated with solar activity. On the other hand, recently Patil et al. (2016) using the same setup observed the percentage occurrence of EPBs during January to April 2012 to vary between 29 and 56 percentage. They also noticed the positive correlation of occurrences and drift of EPBs with solar flux while there is negative correlation of the same with Ap values. However this paper presents the analysis of 351 nights of observations during (2011–2015) of all sky imager data. Study of hourly, seasonal and yearly percentage occurrence of EPBs and their variation with solar and geomagnetic activity, has been made.

2. Instrumentation

2.1. All Sky Imager

The ASI is operated for 7 nights before and after the new moon night. ASI, high resolution (1024 × 1024 pixels) Charge Coupled Device (CCD) based, has 140° field of view (FOV) and covers a angle range of about ±70° around zenith. It corresponds to horizontal distance of about nearly 1220 km in diameter at an altitude of 250 km (Fig. 1). The CCD detector is back-illuminated with an array of 1024 × 1024 pixels (quantum efficiency greater than 95percentage) and 16 bits resolution. Before the operation, dark counts are reduced by thermo-electric cooling (−80 °C) of CCD. The detailed information of ASI has been introduced by Ghodpage et al. (2014). The ASI images are processed using the averaging method which includes different steps. Firstly, we make auto-level

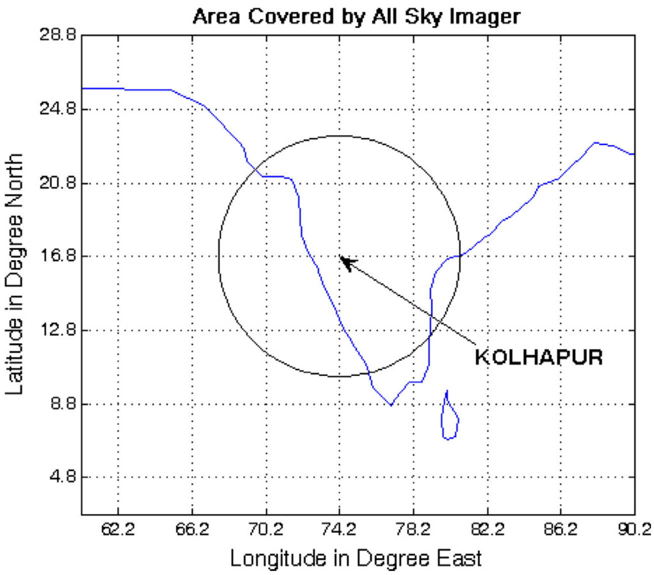

Fig. 1. The all sky imager covers a zenith angle range of about 70° (140° FOV). This corresponds to horizontal distance about nearly 1220 km in diameter at an altitude of 250 km.

(adjusting brightness-contrast) of the raw images in Adobe Photoshop (CS2) to get the EPB structures which are initially faint. We properly align the images with rotating angle 8.2° anticlockwise and then flipped horizontally to get the desired E-W direction. Finally, we average the one hour image data (10 images with 06 min time interval) and subtract individual images from the averaged image to get the final image. This will give a sharp and more clear structures of EPBs aligned in N-S direction. The sequences of processed images are shown in Fig. 2. The yellow arrow indicates the motion of EPBs towards east. The more detailed information of ASI and the processing method can be found in Sharma et al. (2014).

2.2. VHF scintillation

The regular observations of amplitude scintillation at 251 MHz signal transmitted by UFO2 geostationary satellite (71.2° E) has been carried out for last few years at Kolhapur. The system consists of- two identical receivers with eleven element Yagi-Uda antennae, spaced nearly 300 m apart in magnetic east-west direction. The signal is recorded using sampling rate of 20 Hz. Scintillations in the radio signal are calculated by a parameter called S_4-index (S_4). It is the root mean squared standard deviation of intensity of the signal which indicates the strength of amplitude scintillation (Wernik et al. (2004)).

3. Method of data analysis

The occurrence of irregularities (EPBs) at any station situated off the magnetic equator depends on the height to which EPBs develop under E × B (Sushil kumar and Gwal 2000). The geometry of apex height and ray path for the present location indicates that the EPBs must grow over magnetic equator to about 300–400 km to observe the EPBs at this station. During a night of observation, ASI records around 100 images with difference of ~06:00 min for the period of 19:00–05:00 IST. The onset of EPBs can be seen by observing the ASI images.

Here, we have calculated the percentage occurrence as the number of OI 630.0 nm images in which at least one EPB structure is present divided by the total number of images recorded during whole night and multiplied by 100 (Sharma et al., 2014). The one hour images are grouped and the presence of EPBs is observed in every one hour data from 19:00 IST to 05:00 IST for each night. This hourly percentage occurrence has been calculated by observing the number of images for every hour in which EPBs are present during whole night divided by total number of images in that one hour and multiplied by 100. The sample plot of daily percentage occurrence (hourly) for the whole night of 30–31 March 2011 is shown in Fig. 3. The peak of the occurrence lies near mid-night period and gradually decreases towards dawn period. This means that the density of EPBs increases from 20:00 IST (onset) giving peak around mid-night and further decreases towards dawn period.

4. Results and discussion

4.1. The hourly percentage occurrence of EPBs

As discussed in the method of analysis section, the hourly percentage occurrence of EPBs for all the observation nights for all years is calculated and plotted as contours shown in Fig. 4. The ASI is not operated in rainy seasons (June to September). In May, there is no occurrence of EPBs during the observation nights for this location. So, the months from May to September are not included in this analysis. In addition to this, as shown in Fig. 4, the data from October 2013 to March 2014 are not available due to instrument problem. The blue portions in the contours depict the zero occurrences of EPBs and red represents maximum occurrence. In the year 2011 and 2012 (ascending phase of 24th solar cycle), the onset of EPBs was observed around 20:00 IST and it is extended towards remaining course of night with peak around pre-midnight. In February 2013, the occurrence was almost zero. In the year 2014, the occurrence seems to be dense in the November but the occurrence in the December is quite lesser. Moving on to the year 2015 which is near solar maximum year of 24th solar cycle, the occurrence seems to be increased in January to March. Further in October and November, occurrence of EPBs was zero. According to theory of Tsunoda (1985) the ESF season occur at a given location when the sunset terminator is approximately aligned with the geomagnetic flux tubes which mean that the occurrence of EPBs should be maximum in the

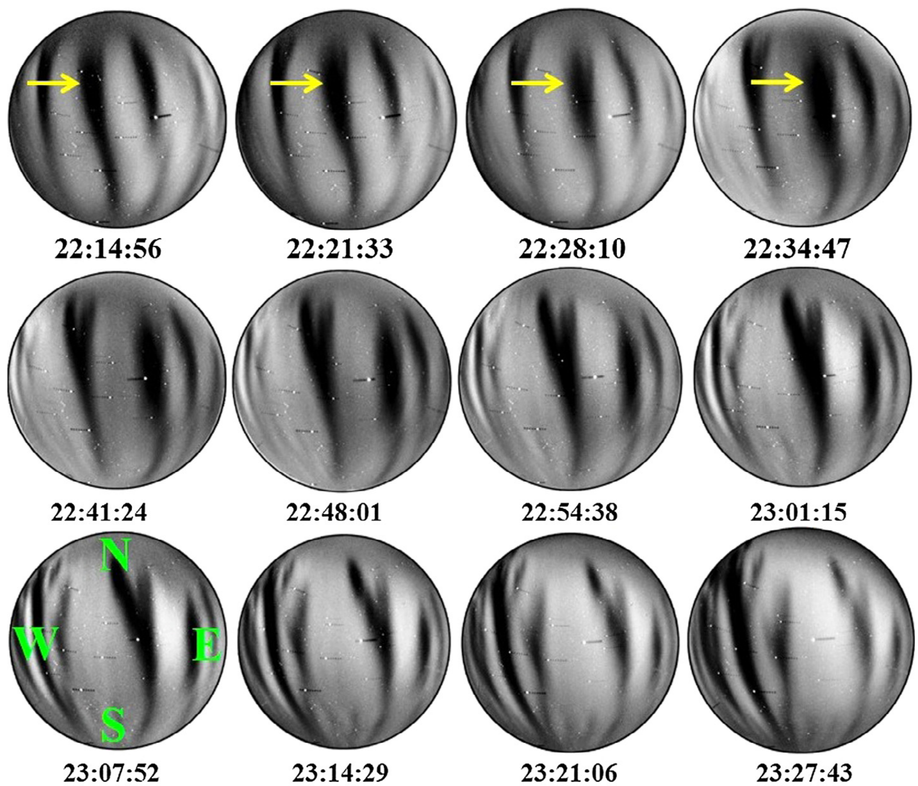

Fig. 2. Sequences of processed images of OI 630.0 nm emissions recorded by ASI on 16–17 Feb 2015, shows signatures of EPBs moving eastward as indicated by yellow horizontal arrows. (For interpretation of the references to colour in this figure legend, the reader is referred to the web version of this article.)

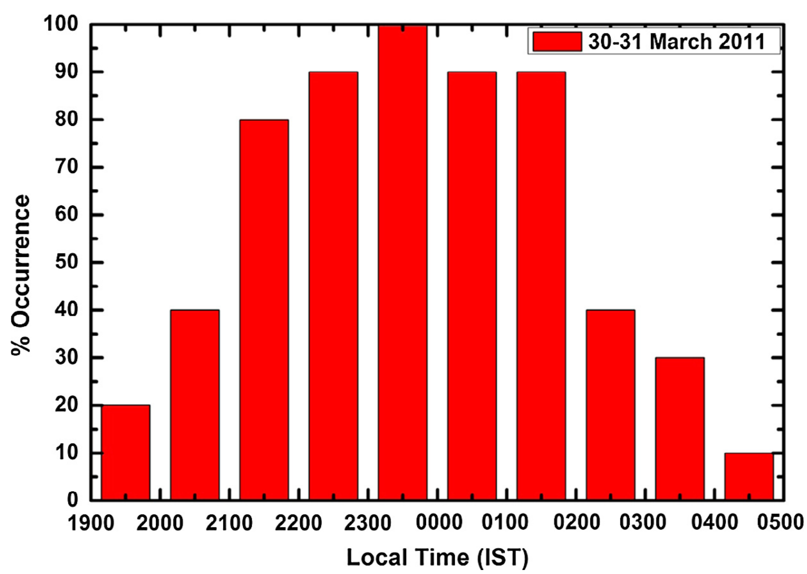

Fig. 3. The daily % Occurrence of EPBs for the night of 30–31 March 2011.

Equinox months. In the October months of every year except 2014 (due to data unavailability) the EPBs are fairly observed. However in the month of October 2015 the EPBs were not observed. From previous literature, it is believed that the small scale structures are present near the steep walls of EPBs which often degrades the communication (Dandekar and Groves 2004). Vijaykumar et al. (2007) studied the plasma bubble induced scintillation (PBI) during the AICPITS campaigns of 1991 and observed the periodic variation in VHF scintillation with saturated S_4 index as 1.2 and dropping to as low as 0.2. This shows that scintillation patch itself has structures. These patches are fairly

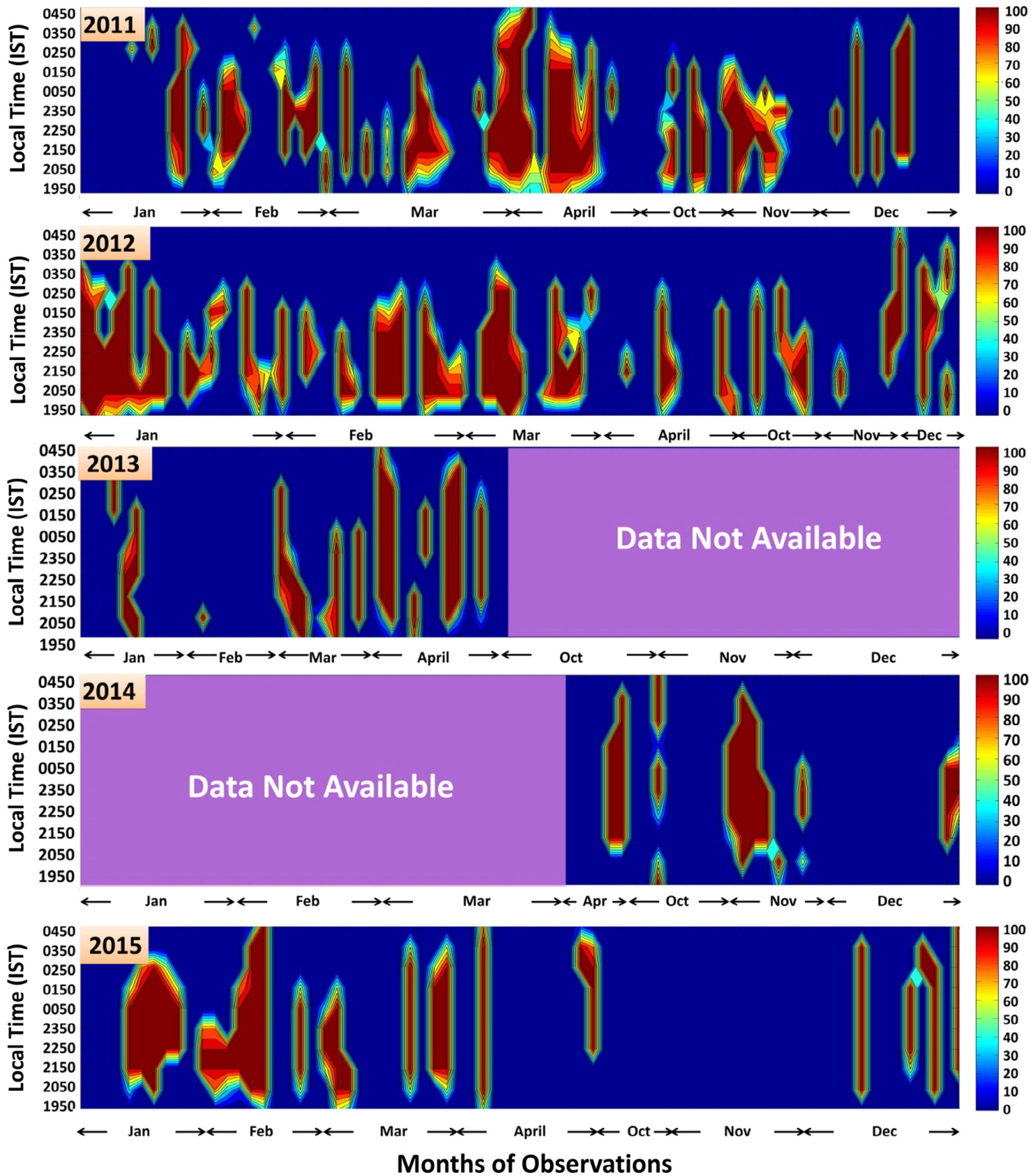

Fig. 4. The hourly % occurrence of EPBs for the days of observations for the five years 2011–2015. Blue portion indicates the absence of EPBs. (For interpretation of the references to colour in this figure legend, the reader is referred to the web version of this article.)

associated with the appearance of periodic EPBs. To understand the cause behind the absence of EPBs on February 2013, December 2014 and October, November 2015, we have checked the scintillation indices (S_4) from the VHF data of same location for the corresponding months. The S4 index can be classified into three categories as, weak ($0.15 \leq S4 \leq 0.3$), moderate ($0.3 \leq S4 \leq 0.5$) and strong ($0.5 \leq S4 \leq 1$) (Bhattacharyya et al. (2003)). We found that S4 indices were moderate (≤ 0.5) in these months. We also observed the S4 indices as stronger

($S4 \geq 0.5$) on the nights in which EPBs are present. Thus, the absence of EPBs could be confirmed due to weak or moderate scintillation over Kolhapur.

Sun et al. (2016) reported the statistical analysis of EPBs using ASI networks over Chinese longitude sector which has nearly similar magnetic and geographic latitudes to our observation site with longitude difference of 20–32°. They observed that, the percentage occurrence of EPBs was 8.3% for 2013 and 17.2% for 2014. It is as low as 10% in November and zero in December months of 2012, 2013 and 2014. This shows discrepancy with that of occurrence studied by Sharma et al. (2014) as well as with the present studies. This discrepancy is might be due to the difference in their longitudes.

4.2. The daily averaged percentage occurrence of EPBs

We have studied the daily averaged percentage occurrence of EPBs and compared it with corresponding 10.7 cm solar flux as shown in Fig. 5. It is calculated by adding the number of images during whole night in which at least one EPB is observed divided by total number of images recorded on that night and multiplied by 100. The summary of data considered for the present study is shown in Table 1. The bottom panel in Fig. 5 is the daily averaged percentage occurrence of EPBs during all the nights of observations from 2011 to 2015. The top panel is the 10.7 cm solar flux for corresponding nights of observations. The yellow colored portion depicts the percentage occurrence for the year 2014 (solar maximum year). In the beginning years 2011 to 2013, the percentage occurrence seems to be fairly associated with 10.7 cm solar flux as reported by Sharma et al. (2014). But in the year 2014, the percentage occurrence seems to be quite suppressed as compared to all other years. Fejer et al. (1999) proposed that the maximum Vp (vertical drift) is larger and smaller under quiet and disturbed conditions respectively during High Solar Activity (HSA) period. In the present observation, in spite of solar maximum year 2014 we observed fewer occurrences of EPBs as compared to all other years. This is due to data loss in October, November and December 2013 and January, February and March 2014. If we had a regular data without loss then we could expect the higher occurrence rate in the year 2014.

4.3. Monthly averaged percentage occurrence of EPBs

We have calculated the monthly averaged percentage occurrence of EPBs and compared it with corresponding monthly averaged 10.7 cm solar flux for the years 2011–2015 as depicted in Fig. 6. The monthly percentage occurrence is calculated by averaging the percentage occurrence of EPBs for all the nights of observation in that month divided by number of observation nights and multiplied by 100. The bottom panel is the monthly averaged percentage occurrence of EPBs. The top panel is the monthly

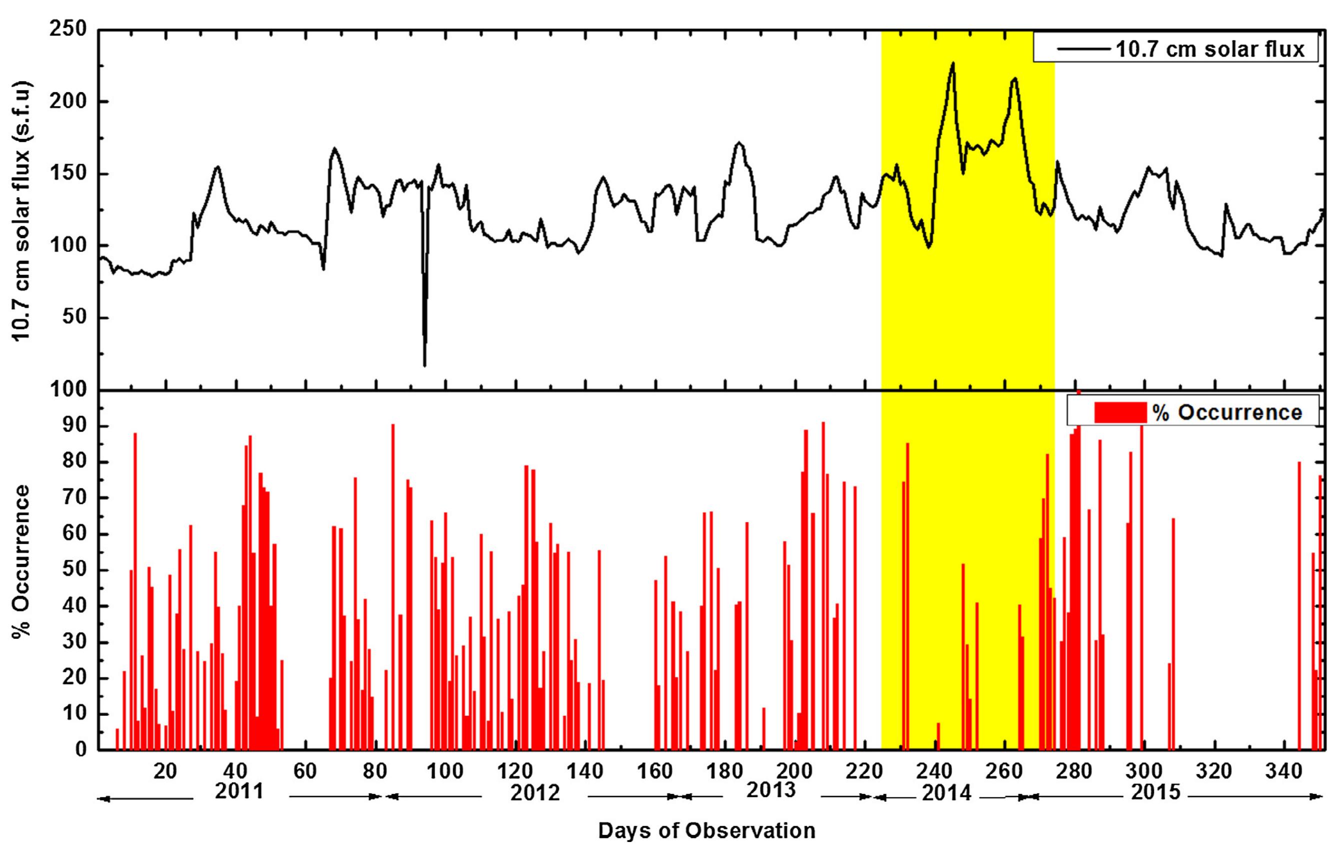

Fig. 5. The daily averaged % occurrence of EPBs with 10.7 cm flux.

Table 1
Summary of five year (2011–2015) observation night's data.

Years	Months	Total number of nights	Total number of images recorded	Event images	Occurrence (%)	Monthly averaged 10.7 cm solar flux (s.f.u)
2011	January	14	1392	195	14.00	85.14
	February	13	1320	362	27.42	84.76
	March	17	1607	499	31.05	127
	April	13	1295	427	32.97	110.61
	May	7	833	0	0	105
	October	7	590	204	34.57	152
	November	9	973	223	22.91	141.11
	December	14	1389	255	18.35	139.14
	Total	**94**	**9399**	**2165**	**22.01 (Avg)**	**118.09 (Avg)**
2012	January	14	1627	574	35.27	133.33
	February	15	1477	432	29.24	105.62
	March	13	1225	380	31.02	104.41
	April	11	1127	116	10.29	122.54
	May	12	1140	0	0	124.16
	October	4	610	167	27.37	138.16
	November	7	737	92	12.48	134.85
	December	8	807	246	30.48	112.25
	Total	**84**	**8750**	**2007**	**22.65 (Avg)**	**121.91 (Avg)**
2013	January	9	852	138	16.19	155.88
	February	10	895	68	7.59	103.2
	March	8	685	187	27.29	118.87
	April	11	957	419	43.78	131.09
	May	10	717	38	3.90	138
	October	–	–	–	–	–
	November	–	–	–	–	–
	December	–	–	–	–	–
	Total	**48**	**4106**	**812**	**13.33 (Avg)**	**129.40 (Avg)**
2014	January	–	–	–	–	–
	February	–	–	–	–	–
	March	–	–	–	–	–
	April	4	412	120	29.12	140.2
	May	7	462	0	0	113.14
	October	9	848	196	23.11	178.11
	November	13	1079	138	12.78	165
	December	6	534	70	13.10	198
	Total	**39**	**3335**	**524**	**15.62 (Avg)**	**158.89 (Avg)**
2015	January	10	838	260	31.02	135.7
	February	11	892	396	44.39	124.72
	March	11	962	286	29.70	121.36
	April	11	941	174	18.49	144.54
	May	14	1274	35	0	108.71
	October	5	446	0	0	115.4
	November	12	1116	0	0	107.58
	December	12	1158	296	25.56	106.53
	Total	**86**	**7627**	**1412**	**18.64 (Avg)**	**120.56 (Avg)**

averaged 10.7 cm solar flux for corresponding observation nights. Due to data loss in October, November and December 2013 and January, February and March 2014, we compared the five year monthly percentage occurrence in such a way that the months (to be compared) are present in all the years. Hence we compared months from January to April for all the years. In this case, we do not have data for January to April 2014 as can be seen in Fig. 6. Sahai et al. (1999) observed the occurrence of EPBs as lesser during LSA (September 1994–January 1998) than during HSA (March 1987–October 1991) over Cachoeira Paulista (22.7 °S, 45.0 °W), Brazil. Here the percentage occurrence is seems to be fairly correlated (with correlation coefficient: 0.35) with solar activity. Overall in Fig. 6, the monthly averaged percentage occurrence of EPBs is positively correlated with solar activity.

4.4. The daily averaged percentage occurrence of EPBs on disturbed nights (Ap > 18)

Amongst all five year data (2011–2015), we have selected the disturbed nights having Ap > 18 (Chavan et al., 2016).

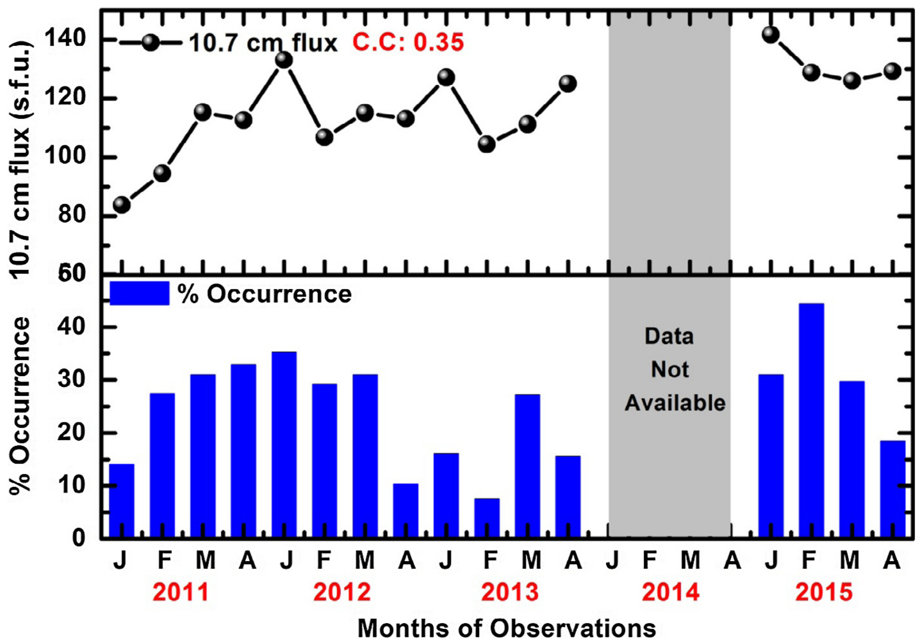

Fig. 6. The monthly averaged % occurrence of EPBs for the period of 2011–2015 along with 10.7 cm flux.

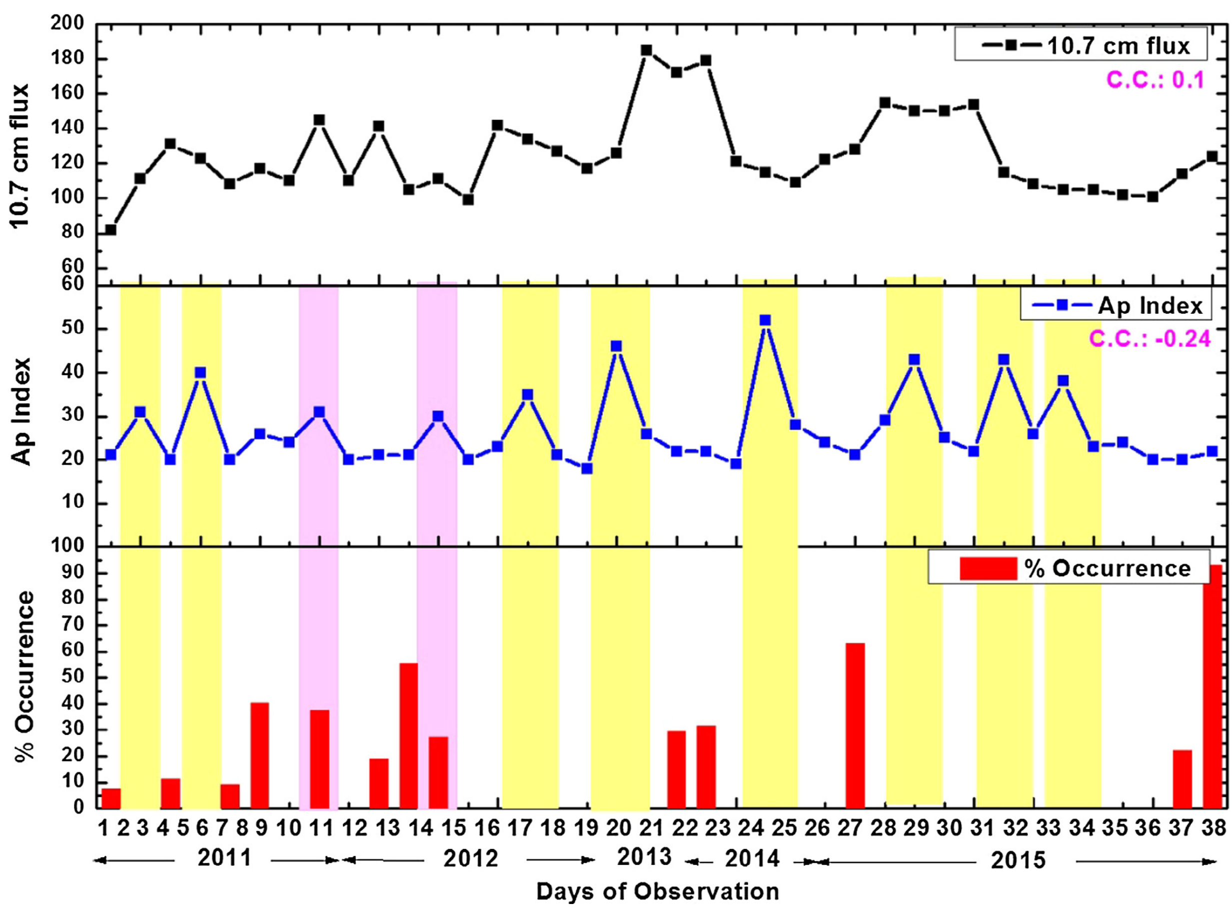

Fig. 7. The daily averaged% occurrence of EPBs on disturbed nights (Ap > 18) amongst five year and its comparison with solar activity (10.7 cm flux).

The daily averaged percentage occurrence on these nights is calculated and compared with corresponding Ap indices (which gives the indication of magnetic activity) and 10.7 cm solar flux as shown in Fig. 7. Daily averaged percentage occurrence is zero (except pink shaded region) for strong magnetic activity, as indicated by yellow bars.

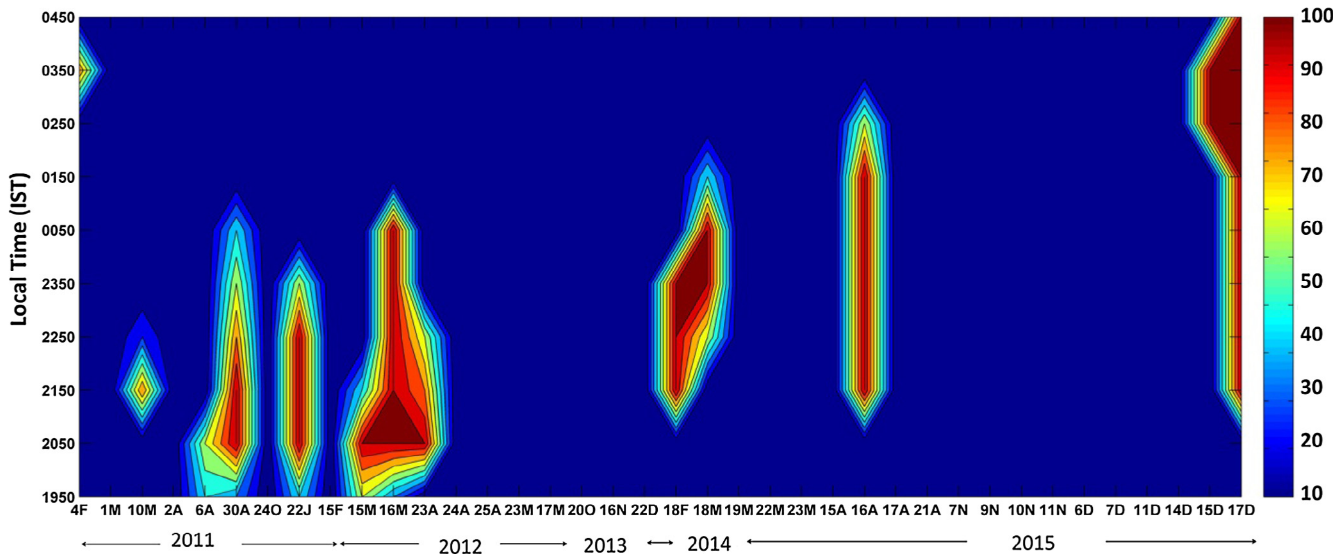

Fig. 8. The hourly % occurrence of EPBs on disturbed nights (Ap > 18) for the period of 2011–2015.

The correlation of Ap values with the occurrence is −0.24. This implies that the magnetic activity (Ap > 18) suppresses the occurrence of EPBs for our location.

During disturbed nights Equatorial spread F (ESF) activity is inhibited due to reduction in eastward electric fields of prereversal enhancement (PRE) (Fejer et al. (1999)). Moreover, the EPB suppression might be occurred due to the prompt penetration electric field of westward polarity which inhibits the PRE (Abdu et al., 2009). Also, it can be stated that a sudden southward turning of the z-component of Bz, from a steady northward pattern, produces a dawn to dusk convection electric field at high latitudes resulting in an under-shielding condition (RamSingh et al., 2015). This makes the strong PRE and subsequently forms ESF over low latitudes. However, the steady southward IMF Bz configuration may not exist for a long and the IMF Bz will turn northward yet again and later over-shielding condition arises. This inhibits the growth of EPBs.

Huang et al. (2001) also found anti-correlation between ESF occurrence rate and enhanced geomagnetic activity during the period of 1989 to 1991 (ascending phase of 22nd solar cycle). During no spread F season Sahai et al. (1994) observed the EPBs over Brazilian sector only under magnetic disturbances, however not all magnetic disturbances produce the EPBs. In Fig. 7, the correlation of 10.7 cm solar flux with the occurrence is 0.1. Here, the occurrence of EPBs under disturbed conditions can be seen, where 10.7 cm solar flux is sufficiently large.

4.5. The hourly percentage occurrence of EPBs on disturbed nights (Ap > 18)

The geomagnetic activity affects the occurrence of irregularities in a manner that depends on local time, season and solar cycle (Hysell and Burcham, 2002). We have calculated the hourly variation in the percentage occurrence of EPBs for all the disturbed nights amongst five years as shown in Fig. 8. In this case, we observed that the EPBs are mostly confined to pre-midnight hours for the year 2011 and 2012 with onset around 19:50 IST. There is no occurrence of EPBs found in the year 2013. Further in the year 2014 and 2015 the onset of EPBs is around 21:00 IST and they are confined to post-midnight period. In the year 2015 which is the near solar maximum year, the EPBs last for long up to 04:50 IST. It should be noted that these EPBs are occurred on the corresponding disturbed nights amongst five years where the solar flux is sufficiently large (>100 s.f.u). Joshi et al. (2012) observed that the EPBs are mostly confined to pre-midnight hours for high solar activity (HSA) (2002–2003) while during low solar activity (LSA) (2007–2009) they are confined to post-midnight and to dawn hours for the 23rd solar cycle over Indian region. In our case, we deal with the disturbed nights only amongst the five year data and it is contradictory to Joshi et al. (2012), as the EPBs are confined to pre-midnight hours for the LSA period of 2011 and 2012 while for the HSA period of 2014 and 2015 they are confined to post-midnight or somewhere towards dawn period.

4.6. Hourly seasonal variation in percentage occurrence of EPBs

For seasonal analysis, the months can be classified as Equinox (March, April, September and October) (E-months), Summer (May to August) (S-months) and Winter (January, February, November and December) (W-months) (Vyas and Dayanandan 2011). Fig. 9 is the hourly averaged percentage occurrence for E and W months for the period of 2011–2015. As discussed in section A), in

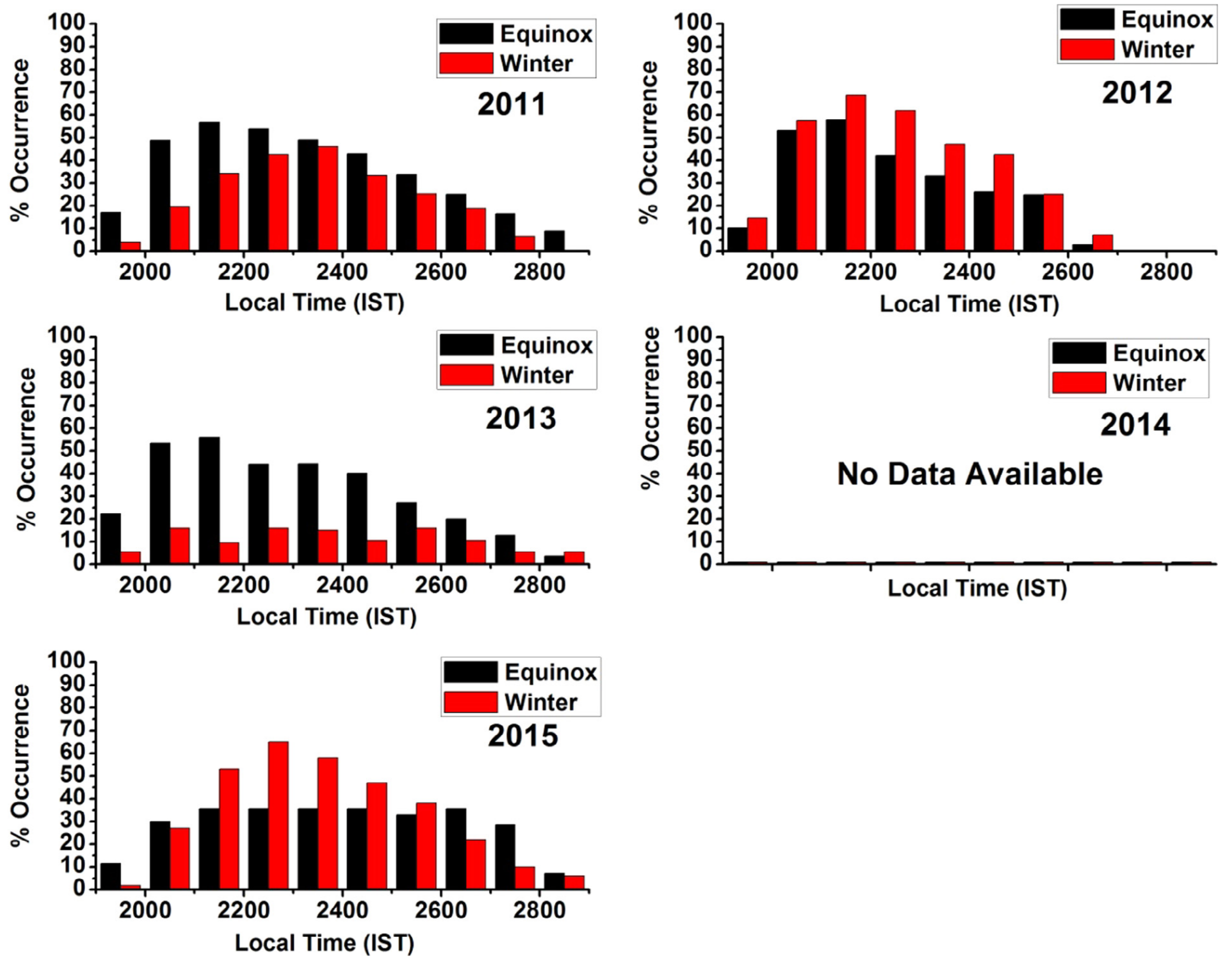

Fig. 9. The hourly % occurrence of EPBs for Equinox (March, April, September, and October) and Winter (January, February, November and December) seasons for the period of 2011–2015.

May the occurrence of EPBs is zero and all other months from summer (i.e. June, July and August) are not suitable for ASI observation at our location due to unfavorable sky conditions and rainy climate. So S-months are not included for seasonal analysis. In this case, due to data loss in October, November, December 2013 and January, February and March 2014, we have considered equinox months as March-April and winter months as January-February to properly compare the seasonal behavior for five years. The hourly percentage occurrence has been calculated by averaging the hourly images for all the nights of observation divided by total number of images during one hour (i.e. 10 images with $\approx$ 06:00 min of difference) and multiplied by 100. Further the final hourly averaged percentage occurrences of each month are averaged to get the hourly seasonal variation.

The black and blue vertical bars represent the hourly percentage occurrence of EPBs for equinox and winter season respectively. For the winter seasons, the hourly percentage occurrence of EPBs is observed to be increased up to 2012. Further it suddenly decreases in year 2013 which is near the maximum peak of 24th solar cycle. While in the equinox months the variation in hourly percentage occurrences of EPBs are fairly remains same up to 2013 and further little decreased in 2015. Sahai et al. (1999) observed the occurrence of EPBs over Brazilian sector as lesser during LSA than during HSA while seasonal pattern were fairly similar for LSA and HSA activity. In our case, during HSA (2013) the seasonal pattern is observed to be suppressed (for winter months) than in LSA. However the occurrence remained steady in equinoctial months. The vertical drift which is the main parameter behind the growth and occurrence of EPBs over low latitude Indian sector can be taken into account for the suppression of EPBs during winter season. Prabhakaran Nayar and Sreehari (2004), using multi-frequency HF Doppler Radar installed at university of Kerala studied the height gradient in vertical plasma drift. They concluded that the mean vertical plasma drift gradient around the PRE exhibits a seasonal variation. In December solstice the magnitude of negative gradient is quite larger, this possibly be the cause behind the fewer occurrences over low latitude Indian sector during December solstices. Also, Sripathi et al. (2016), presented seasonal characteristics of quite time vertical drift by using Canadian Ionosonde at Tirunelveli and their observations suggests that seasonal variations of evening hour vertical drifts are higher during equinox followed by winter and summer. This further suggests that the EPB occurrence might be found lesser during winter and summer months that in equinox months. In present study, in Fig. 9, the occurrences of EPBs are observed to be lesser in winter months (2011, 2013) as compared to equinoctial months.

5. Conclusions

We have analyzed 351 nights ASI data from five years 2011–2015 to study the variation in the percentage occurrences of EPBs as hourly, daily, seasonally and yearly from low latitude station Kolhapur (16.8 °N, 74.2 °E). The results are listed below.

(1) The onset of EPBs is generally occurred around 20:00 IST and extended well towards dawn period with a peak around mid-night.
(2) The daily averaged percentage occurrence of EPBs for the year 2014 (a solar maximum year) is seen to be somewhat suppressed. This might be due to data loss in October, November and December 2013 and January, February and March 2014. However, the overall occurrence of EPBs (Daily averaged) is fairly associated with 10.7 cm solar flux for all other years.
(3) The magnetic activity ($Ap > 18$) suppresses the occurrence of EPBs at Kolhapur station. We suggest that the EPB suppression might be occurred due to the prompt penetration electric field of westward polarity which inhibits the PRE (Abdu et al., 2009).
(4) It is interesting to note that, during the disturbed nights ($Ap > 18$), EPBs are confined to pre-midnight hours for the period of 2011 and 2012 while for the period of 2014 and 2015 they are confined to post-midnight or fairly towards dawn period. This aspect needs more clarification in future studies.
(5) The hourly percentage occurrence in Equinox months is remains almost same up to 2013 (ascending phase of 24th solar cycle). However, the hourly percentage occurrences in winter months were found to be decreased in the year 2011 and 2013.

Acknowledgement

One of the authors Mr. O. B. Gurav is thankful to UGC-BSR for financial support. We are thankful to the NOAA-GOES for providing the data of solar and geomagnetic indices over the Internet (ftp.swpc.noaa.gov/pub/warehouse). We are thankful to IIG Mumbai, for providing data of OI 630.0 nm emission. This data has been recorded under the scientific collaboration between Indian Institute of Geomagnetism (I.I.G.), Navi Mumbai and Shivaji University, Kolhapur (S.U.K).

References

Abalde, J.R., Sahai, Y., Fagundes, P.R., Becker-Guedes, F., Bittencourt, J.A., Pillat, V.G., Lima, W.L.C., Candido, C.M.N., De Freitas, T.F., 2009. Day-to-day variability in the development of plasma bubbles associated with geomagnetic disturbances. J. Geophys. Res. Sp. Phys. 114, 1–11.

Abdu, M.A., Kherani, E.A., Batista, I.S., Sobral, J.H.A., 2009. Equatorial evening prereversal vertical drift and spread F suppression by disturbance penetration electric fields. Geophys. Res. Lett. 36, L19103. https://doi.org/10.1029/2009GL039919.

Bhattacharyya, A., Groves, K.M., Basu, S., Kuenzler, H., Valladares, C. E., Sheehan, R., 2003. L-band scintillation activity and space-time structure of low-latitude UHF scintillations. Radio Sci. 38, 1–9. https://doi.org/10.1029/2002RS002711.

Chakraborty, S.K., DasGupta, A., Ray, S., Banerjee, S., 1999. Long-term observations of VHF scintillation and total electron content near the crest of the equatorial anomaly in the Indian longitude zone. Radio Sci. 34, 241–255.

Chavan, G.A., Sharma, A.K., Gurav, O.B., Gaikwad, H.P., Nade, D.P., Nikte, S.S., Ghodpage, R.N., Patil, P.T., 2016. Dependence of coherence scales of ionospheric scintillation patterns on magnetic activity. Mapan - J. Metrol. Soc. India 1–7, 2016. https://doi.org/10.1007/s12647-016-0191-3.

Dandekar, B.S., Groves, K.M., 2004. Using ionospheric scintillation observations for studying the morphology of equatorial ionospheric bubbles. Radio Sci. 39. https://doi.org/10.1029/2003RS003020.

Ghodpage, R.N., Taori, A., Patil, P.T., Gurubaran, S., Sripathi, S., Banola, S., Sharma, A.K., 2014. Simultaneous optical measurements of equatorial plasma bubble (EPB) from Kolhapur (16.8°N, 74.2°E) and Gadanki (13.5°N, 79.2°E). J. Atmos. Solar-Terrest. Phys. 121, 196–205.

Fagundes, P.R., Sahai, Y., Batista, I.S., Abdu, M.A., Bittencourt, J.A., Takahashi, H., 1999. Observations of day-to-day variability in precursor signatures to equatorial F-region plasma depletions. Ann. Geophys. 17, 1053–1063.

Fejer, B.G., Scherliess, L., de Paula, E.R., 1999. Effects of the vertical plasma drift velocity on the generation and evolution of equatorial spread-F. J. Geophys. Res. 104, 19859–19869.

Haase, J.S., Dautermann, T., Taylor, M.J., Chapagain, N., Calais, E., Pautet, D., 2011. Propagation of plasma bubbles observed in Brazil from GPS and airglow data. Adv. Sp. Res. 47, 1758–1776.

Huang, C.Y., Burke, W.J., Machuzak, J.S., Gentile, L.C., Sultan, P.J., 2001. DMSP observations of equatorial plasma bubbles in the topside ionosphere near solar maximum. J. Geophys. Res. 106, 8131. https://doi.org/10.1029/2000JA000319.

Hysell, D.L., Burcham, J.D., 2002. Long term studies of equatorial spread F using the JULIA radar at Jicamarca. J. Atmos. Solar-Terrest. Phys. 64, 1531–1543.

Iyer, K.N., Jivani, M.N., Abdu, M.A., Joshi, H.P., Aggarwal, M., 2006. Power spectral studies of VHF ionospheric scintillations near the crest of the equatorial anomaly in India. Indian J. Radio Sp. Phys. 35, 234–241.

Joshi, L.M., Patra, A.K., Rao, S.V.B., 2012. Equatorial F-region irregularities during low and high solar activity conditions. Indian J. Radio Sp. Phys. 41, 208–219.

Kumar, Sanjay, 2017. Morphology of equatorial plasma bubbles during low and high solar activity years over Indian sector. Astrophys. Space Sci. 362, 93. https://doi.org/10.1007/s10509-017-3074-3.

Kumar, S., Gwal, A.K., 2000. VHF ionospheric scintillations near the equatorial anomaly crest: solar and magnetic activity effects. J. Atmos. Solar-Terrest. Phys. 62, 157–167.

Makela, J.J., Miller, E.S., 2008. Optical observations of the growth and day-to-day variability of equatorial plasma bubbles. J. Geophys. Res. Sp. Phys. 113, 1–7.

Mendillo, M., Baumgardner, J., Pi, X., Sultan, P.J., Tsunoda, R., 1992. Onset conditions for equatorial spread F. J. Geophys. Res. 97, 13865–13876.

Mukherjee, G.K., Carlo, L., Mahajan, S.H., Patil, P.T., 1998. First results of all-sky imaging from India. Earth, Planets Sp. 50, 119–127.

Nade, D.P., Sharma, A.K., Nikte, S.S., Patil, P.T., Ghodpage, R.N., Rokade, M.V., Gurubaran, S., Taori, A., Sahai, Y., 2013. Zonal velocity of the equatorial plasma bubbles over Kolhapur, India. Ann. Geophys. 31, 2077–2084.

Narayanana, V.L., Gurubaran, S., Berlin Shiny, M.B., Emperumal, K., Patil, P.T., 2017. Some new insights of the characteristics of equatorial plasma bubbles obtained from Indian region. J. Atmos. Solar Terr. Phys. 156, 80–86.

Patil, P.T., Ghodpage, R.N., Taori, A.K., Patil, R.P., Gurubaran, S., Nikte, S.N., Nade, D.P., Sharma, A.K., Banola, S., Narayanan, V.L., Siingh, D., 2012. The study of equatorial plasma bubble during January to April 2012 over Kolhapur (India). Ann. Geophys. 59, 2016. https://doi.org/10.4401/ag-6868.

Patra, A.K., Tiwari, D., Sripathi, S., Rao, P.B., Sridharan, R., Devasia, C. V., Viswanathan, K.S., Subbarao, K.S.V., Sekar, R., Kherani, E.A., 2005. Simultaneous radar observations of meter-scale F region irregularities at and off the magnetic equator over India. J. Geophys. Res. 110, A02307. https://doi.org/10.1029/2004JA010565.

Patra, A.K., Srinivasulu, P., Pavan Chaitanya, P., Durga Rao, M., Jayaraman, A., 2012. First results on low-latitude E and F region irregularities obtained using the Gadanki Ionospheric Radar Interferometer. J. Geophys. Res. Space Phys. 119(10), 276–310, 293, http://dx.doi.org/10.1002/2014JA020604.

Pimenta, A.A., Fagundes, P.R., Bittencourt, J.A., Sahai, Y., Gobbi, D., Medeiros, A.F., Taylor, M.J., Takahashi, H., 2001. Ionospheric plasma bubble zonal drift: A methodology using OI 630 mn all-sky imaging systems. Adv. Sp. Res. 27, 1219–1224.

Prabhakaran Nayar, S.R., Sreehari, C.V., 2004. Investigation of height gradient in vertical plasma drift at equatorial ionosphere using multifrequency HF Doppler radar. J. Geophys. Res. 109, A12308. https://doi.org/10.1029/2004JA010641.

Rama Rao, P.V.S., Gopi Krishna, S., Niranjan, K., Prasad, D.S.V.V.D., 2006. Temporal and spatial variations in TEC using simultaneous measurements from the Indian GPS network of receivers during the low solar activity period of 2004 & 2005. Ann. Geophys. 24, 3279–3292.

Ramsingh, Sripathi S., Sreekumar, Sreeba, Banola, S., Emperumal, K., Tiwari, P., Kumar, Burudu Suneel, 2015. Results from a chain of ground-based observations over Indian sector. J. Geophys. Res. Sp. Phys. 120 (10864–10882), 2015. https://doi.org/10.1002/2015JA021509.

Sahai, Y., Aarons, J., Mendillo, M., Baumgardner, J., Bittencourt, J.A., Takahashi, H., 1994. OI 630 nm imaging observations of equatorial plasma depletions at 16° S dip latitude. J. Atmos. Terr. Phys. 56, 1461–1475. https://doi.org/10.1016/0021-9169(94)90113-9.

Sahai, Y., Fagundes, P.R., Bittencourt, J.A., 1999. F-region plasma depletions. Adv. Space Res. 24, 1477–1480.

Sharma, A.K., Nade, D.P., Nikte, S.S., Patil, P.T., Ghodpage, R.N., Vhatkar, R.S., Rokade, M.V., Gurubaran, S., 2014. Occurrence of equatorial plasma bubbles over Kolhapur. Adv. Sp. Res. 54, 435–442.

Sinha, H.S.S., Misra, R.N., Chandra, H., Raizada, S., Dutt, N., Vyas, G. D., 1996. Multi-wavelength optical imaging of ionospheric plasma depletions. IJRSP-Indian J. Radio Sp. Phys. 25, 44–52.

Sripathi, S., Singh, Ram., Banola, S., Sreekumar, Sreeba., Emperumal, K., Selvaraj, C., 2016. Characteristics of the equatorial plasma drifts as obtained by using Canadian Doppler ionosonde over southern tip of India. J. Geophys. Res. Sp. Phys. 121. https://doi.org/10.1002/6JA023088.

Sun, L., Xu, J., Wang, W., Yuan, W., Li, Q., Jiang, C., 2016. A statistical analysis of equatorial plasma bubble structures based on an all-sky airglow imager network in China. J. Geophys. Res. Sp. Phys., 5009–5021 https://doi.org/10.1002/2016JA022950.

Taori, A., Jayaraman, A., Kamalakar, V., 2013. Imaging of mesosphere–thermospheric airglow emissions over Gadanki (13.51° N, 79.21° E)-first results. J. Atmos. Solar Terr. Phys. 93, 21–28.

Taori, A., Parihar, N., Ghodpage, R., Dashora, N., Sripathi, S., Kherani, E.A., Patil, P.T., 2015. Probing the possible trigger mechanisms of an equatorial plasma bubble event based on multistation optical data. J. Geophys. Res. Space Phys. 120, 8835–8847.

Tsunoda, R.T., 1985. Control of the seasonal and longitudinal occurrence of equatorial scintillations by the longitudinal gradient in integrated Eregion Pedersen conductivity. Jgr 90, 447–456.

Vijayakumar, P.N., Tyagi, T.R., Singh, L., Chandra, H., Vyas, G.D., Rao, D.R.K., Pathan, B.M., Iype, A., Ramsekaran, B., Naidu, A., Sadique, S.M., Iyer, K.N., Pathak, K.N., Gwal, A.K., Kumar, S., Singh, R.P., Singh, U.P., Singh, B., Kumar, P., Navneeth, G.N., Koparkar, P.V.S., Ramarao, P.V.S., Jaychandran, P.T., Sriram, P., Sethuraman, R., Dasgupta, A., Basu, K., Rastogi, R.G., 2007. Some features of plasma bubble induced scintillations during the AICPITS campaigns of 1991. Indian J. Radio Sp. Phys. 36, 91–102.

Vyas, B.M., Dayanandan, B., 2011. Nighttime VHF ionospheric scintillation characteristics near the crest of Appleton anomaly station, Udaipur (24.6°N, 73.7°E). Indian J. Radio Sp. Phys. 40, 191–202.

Wernik, A.W., Alfonsi, L., Materassi, M., 2004. Ionospheric irregularities, scintillation and its effect on systems. Acta Geophys. Pol. 52, 237–249.

Whalen, J.A., 2002. Dependence of equatorial bubbles and bottom side spread F on season, magnetic activity, and EXB drift velocity during solar maximum. J. Geophys. Res. 107 (A2), 1024. https://doi.org/10.1029/2001ja000039, 2002.

Xiong, C., Park, J., Luhr, H., Stolle, C., Ma, S.Y., 2010. Comparing plasma bubble occurrence rates at CHAMP and GRACE altitudes during high and low solar activity. Ann. Geophys. 28, 1647–1658.